Insect Biochemistry and Molecular Biology 110 (2019) 1–9

Contents lists available at ScienceDirect

Insect Biochemistry and Molecular Biology

journal homepage: www.elsevier.com/locate/ibmb

Functional analysis and characterization of antimicrobial phosphatidylethanolamine-binding protein BmPEBP in the silkworm *Bombyx mori*

Muya Tang[a,b,c], Zhaoming Dong[a,c], Pengchao Guo[a,c], Yan Zhang[a,c], Xiaolu Zhang[a,b,c], Kaiyu Guo[a,b,c], Lingna An[a,b,c], Xinyang Liu[a,b,c], Ping Zhao[a,c,*]

[a] *Biological Science Research Center, Southwest University, Chongqing, 400716, China*
[b] *State Key Laboratory of Silkworm Genome Biology, Southwest University, Chongqing, 400716, China*
[c] *Chongqing Key Laboratory of Sericultural Science, Chongqing Engineering and Technology Research Center for Novel Silk Materials, Southwest University, Chongqing, 400716, China*

ARTICLE INFO

Keywords:
Silkworm
Phosphatidylethanolamine-binding protein
Silk gland
Evolution
Structure
Expression pattern
Antifungal activity

ABSTRACT

Phosphatidylethanolamine-binding proteins (PEBPs) are a class of highly conserved, biologically diverse proteins, which are widely distributed in plants, insects, and mammals. In this study, a *Bombyx mori* PEBP (*BmPEBP*) gene was reported, which encodes a protein composed of 209 amino acid residues. BmPEBP includes a predicted signal peptide, indicating that it is an extracellular protein, which differs from the cytoplasmic PEBPs of plants and mammals. Recombinant soluble BmPEBP was successfully synthesized using a prokaryotic expression system and was then purified effectively by Ni^{2+}-NTA affinity chromatography and gel filtration. Far-ultraviolet circular dichroism spectra indicated that BmPEBP had a well-defined β-sheet structure, with the β-sheet content accounting for about 41% of the protein. BmPEBP had a relatively stable structure at temperatures ranging from 15 °C to 57.5 °C. The Tm, ΔH, and ΔS of BmPEBP were 62.27 °C ± 0.14 °C, 570.10 ± 0.17 kJ/mol, and 1.70 ± 0.03 KJ/(mol·K), respectively. Homology modeling analysis suggested that the active sites of BmPEBP were conserved, comprising Pro96, His111, and His143. Quantitative real-time PCR showed that *BmPEBP* was highly expressed in the silk gland and had very low expression in other tissues. However, *BmPEBP* expression was significantly upregulated in the larval fat body after infection with two kinds of fungi, *Beauveria bassiana* and *Candida albicans*. Moreover, *in vitro* fungal inhibition tests showed that BmPEBP could significantly inhibit the sporular growth of *Saccharomyces cerevisiae*, *C. albicans*, *B. bassiana*, and *Aspergillus fumigatus*. To our knowledge, this is the first report to reveal the antifungal role of a PEBP in insects.

1. Introduction

Phosphatidylethanolamine-binding proteins (PEBPs) are proteins of about 23 kDa, which were originally purified as cytosolic proteins from the bovine brain (Bernier and Jollès, 1984). PEBPs have been identified in diverse organisms such as plants (Bradley et al., 1997), parasites (Trottein and Cowman, 1995), nematodes (Gems et al., 1995), insects (Pikielny et al., 1994), and mammals (Tohdoh et al., 1995). The structure of PEBPs is highly conserved in various species. X-ray crystal diffraction studies have shown that the human PEBP protein comprises nine β-sheets and four α-helices. Its main feature is its large central β-folding area, which exists in the form of a Greek-key motif with six β-folded sheets, forming a compact structure (Banfield and Brady, 2000a; Banfield et al., 1998a; Mima et al., 2005; Simister et al., 2010). The protein surface has a narrow cavity adjacent to the hypothetical membrane-bound surface and is considered an important ligand-binding site.

PEBPs have been widely found in mammals, including humans, cattle, rats, and sheep. It has been found in the brain, liver, spleen, stomach, and muscle, with various biological functions (Keller et al., 2004; Ojika, 2000). Hengst et al. (2001) identified a PEBP protein named nexin-1 in the brain of mice, which exhibits wide inhibitory activities against several serine proteases, including thrombin, neuropsin, and chymotrypsin (Hengst et al., 2001). Yeung et al. (2001) found that PEBP indirectly or directly interferes with MEK phosphorylation by binding to Raf-1 or MEK, blocking downstream mitogen-activated protein kinase (MAPK) signaling (Yeung et al., 2000). In addition, Gibbons et al. (2005) discovered that PEBP is a decapacitation

* Corresponding author. Biological Science Research Center, Southwest University, Chongqing, 400716, China.
E-mail address: zhaop@swu.edu.cn (P. Zhao).

https://doi.org/10.1016/j.ibmb.2019.03.011
Received 15 October 2018; Received in revised form 26 March 2019; Accepted 28 March 2019
Available online 31 March 2019
0965-1748/

factor (DF) receptor in mice, which is distributed outside the cell, mainly in the acrosome and flagella of sperm, and it activates sperm by binding to DF (Gibbons et al., 2005). Interestingly, the PEBP from the bovine brain and human brain can bind to many kinds of small-molecule agents such as ATP, opioids, acetate, phosphate, dimethyl arsenate, and phosphatidylethanolamine (Banfield et al., 1998b; Simister et al., 2010).

PEBPs have also been identified in insects by proteomics methods. In 2003, Sofia et al. identified the PEBP1 protein CG18594 in the hemolymph of *Drosophila melanogaster*. Moreover, PEBP was demonstrated to be related to the innate immune defense in insects, especially against bacterial infection (Guedes et al., 2003; Karlsson et al., 2004; Vierstraete et al., 2004). The *PEBP1* gene was found to be upregulated after *D. melanogaster* was infected with bacteria; the protein concentration of PEBP1 increased 6.56-fold in hemolymph after infection. Reumer et al. (2009) studied bacteria-infected *D. melanogaster* in which PEBP1 was overexpressed, and found that the survival rate of PEBP-overexpressed *D. melanogaster* was higher than that of the control group (Reumer et al., 2009). In 2015, Su et al. identified a *PEBP* gene in the silk gland of *Sylepta derogata* by using RNA-seq (Su et al., 2015). In the same year, Zhang et al. identified PEBP (BmPEBP) in the *B.mori* cocoon by a proteomics approach (Zhang et al., 2015). BmPEBP shared common features with some reported silk proteins, including protease inhibitors and seroins, all of which have low molecular weights and high expression in the middle silk gland. (Dong et al., 2013; Guo et al., 2016; Li et al., 2012, 2015a, 2015b). Since protease inhibitors and seroins were reported as antimicrobial proteins, we wonder if BmPEBP also play an antimicrobial role in the silk. In this study, we analyzed the sequence evolution, structural characterization, and expression pattern of BmPEBP. In addition, we also expressed recombinant BmPEBP and studied its physicochemical properties.

2. Materials and methods

2.1. Sample preparation

Silkworms of *B. mori* strain Dazao (maintained in the State Key Laboratory of Silkworm Genome Biology at the Southwest University of China) were reared on fresh mulberry leaves at 25 °C, 75% ± 5% relative humidity, and a photoperiod of 12 h light/12 h dark. Four fungal species—*A. fumigatus*, *C. albicans*, *B. bassiana*, and *S. cerevisiae* (Bei Chuang Biological, China)—were cultured on potato dextrose agar (PDA) medium for 15 days at 30 °C. Fungal conidia were harvested from the above culture and suspended in distilled water containing 0.05% (vol^{-1}) Tween-80 at a concentration of 1×10^5 conidia mL^{-1} after being filtered through sterilized absorbent cotton. Fungal spore liquid (10 μL) was injected into each larva on day 3 of the fifth instar, and larvae injected with sterile PBS were set as the control group. The hemolymph and fat bodies of 25 silkworms were collected from each group 6, 12, 18, and 24 h after injection. The hemolymph was collected in a centrifuge tube containing phenylthiourea and then centrifuged at 4 °C for 10 min at 1000 × *g* to remove blood cells. The same method was used to collect hemolymph from silkworm larvae infected by the bacteria *Escherichia coli* and *Staphylococcus aureus* (Bei Chuang Biological, China). Material from each group was divided into three tubes and stored at −80 °C with liquid nitrogen.

2.2. Bioinformatics analysis

The nucleotide sequences and amino acid sequences of PEBPs were downloaded from the silkworm genome database SilkDB (http://silkworm.swu.edu.cn/silkdb) and NCBI (https://www.ncbi.nlm.nih.gov/). According to the silkworm PEBP protein sequence reported by Dong et al. (2013), the protein sequence of BmPEBP was used to blast against the NCBI non-redundant protein database (blastp, E value: e−5). More than 200 PEBP homologs were identified, of which 60 PEBPs from 20 insect species, 20 mammal species and 20 plant species were chosen to construct the phylogenetic tree. The secondary and tertiary structures of BmPEBP were predicted by Psipred (http://bioinf.cs.ucl.ac.uk/psipred/). Multiple sequence alignment was performed by ClustalX and rendered by ESPript 3.0 using default parameters. A phylogenetic tree was constructed by MEGA 6.0 using a neighbor-joining method.

2.3. Quantitative real-time PCR

Total RNAs were extracted from the head, cuticle, fat body, hemolymph, gonads, Malpighian tubules, midgut, and silk glands on day 3 of the fifth instar by using an RNApure total RNA rapid extraction kit. Reverse transcription into cDNA was performed using M-MLV reverse transcriptase (Invitrogen, USA). Real-time quantitative PCR (qPCR) was performed in a qTOWER2.2 qPCR machine (Analytikjena Biometra, Germany). Each amplification reaction was performed in a total volume of 20 μL containing 150 ng of cDNA (2 μL), 10 μL SYBR Premix Ex TaqII(TaKaRa, Japan), and 0.4 μM primers (forward primer: 5′-TGT GCG TGC TAT AGA AAC-3′, reverse primer: 5′-CAG GCA AGC GTT GTC GT-3′). Real-time qPCR was performed by using the following program: initial denaturation at 95 °C for 30s, followed by 40 cycles of denaturation at 95 °C for 10 s, annealing at 60 °C for 30 s, and extension at 72 °C for 35 s. To calculate the relative expression level of *BmPEBP*, the expression value of *BmPEBP* gene and *sw22934* gene (a housekeeping gene) was recorded as C_t and C_{sw}, respectively. The relative expression value (Cr) of *BmPEBP* gene was then calculated using the following formula: $Cr = 2^{-\triangle(Ct - Csw)}$.

2.4. Protein expression and purification

The coding region of the *BmPEBP* gene without the signal peptides was PCR-amplified using a sense primer (5′-CGC GGA TCC ATG TCT ACC GTA GCG AGG TC-3′) and an antisense primer (5′-ATT TGC GGC CGC TTA AAC ACC GAG TTG GTT C-3′). The purified PCR product was inserted into *Bam*HI and *Not*I (TaKaRa) sites in a reformed expression plasmid of pET28a. The resultant plasmid was transformed into *E. coli* strain BL21 (DE3) (TransGen Biotech, China) and expressed as a fusion protein, which was induced with 0.1 mM IPTG. The *E. coli* cells were lysed in binding buffer (20 mM Tris-HCl, 200 mM NaCl, pH 7.5) by sonication. After centrifugation (12,000 × *g*, 4 °C, 25 min), the separated lysate was subjected to 15% reduced SDS-PAGE.

The lysate supernatant from 400 mL cultures was loaded onto a 2 mL Ni2+-NTA affinity chromatography column, which was equilibrated with binding buffer. The bound protein was eluted with gradient elution buffer (0, 20, 50, 75, 100, 200, 300, and 500 mM imidazole in binding buffer) and then loaded onto a HiLoad 16/60 Superdex 200 column (GE Healthcare) pre-equilibrated with 20 mM phosphate (pH 7.5). The purified recombinant BmPEBP was mixed with SDS-PAGE loading buffer with a reducing agent (β-mercaptoethanol) and analyzed using 15% protein gels. The purified protein was estimated by SDS-PAGE and then stored at −80 °C. The protein concentration of purified BmPEBP was measured using a Bradford assay kit (Beyotime, China).

2.5. Western blot analysis

The samples were separated using 12% SDS- PAGE and then transferred to polyvinylidene fluoride membranes, which were treated with 5% blocking protein powder in 50 mM Tris-HCl (pH 8.0), 500 mM NaCl, and 0.2% Tween 20 (TBST) for 2 h and reacted with the rabbit anti-BmPEBP (Zeheng, China) in TBST for 1.5 h at room temperature. The membranes were washed with TBST three times for 10 min each, and then incubated with the secondary goat anti-rabbit IgG conjugated with horseradish peroxidase (Beyotime) in TBST for 1.5 h at room temperature; the TBST wash was then repeated. Protein signals were detected using the ESLTM Advance Western Blotting Kit (GE

Healthcare).

2.6. Circular dichroism spectroscopy

Far-ultraviolet (far-UV) circular dichroism (CD) spectra were recorded on a MOS-500 CD spectrometer (Bio-Logic, France) with a 0.05 cm quartz cell at 25 °C at 190–250 nm using standard procedures. BmPEBP concentration was 0.025 mg/mL in 20 mM PBS and 200 mM NaCl (pH 8.0). The effects of pH on the secondary structure of BmPEBP were recorded in a pH range of 3–11. The thermal denaturation of BmPEBP (concentration, 0.025 mg/mL) was performed from 5 °C to 95 °C at a gradient of 2.5 °C. The mean residue ellipticities at 216 nm were used to characterize the structural changes of BmPEBP induced by temperature and pH after subtracting for baseline corrections.

2.7. Assay for protein inhibitory activity

Protease inhibition assays were conducted by measuring the residual hydrolytic activity. BmPEBP (100 μg) was preincubated with protease (10 μg) in 100 μL Fluoro™ assay buffer (100 mM Tris-HCl and 20 mM $CaCl_2$, pH 8.0) for 30 min at 37 °C, and then 100 μL FITC-casein substrate (G-Biosciences) buffer was added (Thermo Fisher Scientific, USA), followed by incubation at 37 °C in darkness for 60 min. Substrate hydrolysis was monitored by measuring the excitation at 485 nm and emission at 535 nm in 96-well fluorometer-compatible titer plates. The inhibition of proteases by BmPEBP was assessed using the following formula: % inhibition = (1 − residual enzyme activity/enzyme activity without inhibitor) × 100.

2.8. Growth inhibition assay of fungal spores

Growth inhibition assays were performed in flat-bottom 96-well plates (Corning, USA). Each well was filled with 300 μL of potato liquid medium containing fungal conidia at a final concentration of 1×10^5 conidia mL^{-1}. The culture medium contained chloramphenicol to prevent bacterial infection. We have used a BmPEBP protein with a concentration of 0.1 mg/mL for denaturation at 65 °C for 20 min. The BmPEBP protein obtained after heat denatured is abbreviated as “hdPEBP”. Sterile hdPEBP (heat denatured BmPEBP) and EDTA were used as negative and positive controls, respectively, and BmPEBP protein (0.1 mg/mL) served as the experimental group. Microplates were incubated at 30 °C, and fungal growth was observed by monitoring the absorbance at 595 nm after culturing for 0, 12, 24, 36, and 48 h.

2.9. Growth inhibition assay of bacteria

Growth inhibition assays for bacteria were performed in flat-bottom 96-well plates. Antimicrobial activity of recombinant BmPEBP was estimated against gram-negative *E. coli* and gram-positive *S. aureus*. Each well was filled with 200 μL of LB medium containing bacterial. After cultured in LB medium to OD600 of 0.2. Sterile hdPEBP and EDTA were used as negative and positive controls, respectively, and BmPEBP protein (0.1 mg/mL) was the experimental group. Microplates were incubated at 30 °C, and bacterial growth was observed by monitoring the absorbance at 595 nm after culturing for 0, 6, 12, 18, and 24 h.

3. Results

3.1. Bioinformatics analysis and prokaryotic expression of BmPEBP

The ORF of the *BmPEBP* gene was found to encode a protein composed of 209 amino acid residues. The predicted signal peptide of BmPEBP is observed at the N-terminal 26 amino acid sequence (Fig. 1), indicating that PEBP might be secreted into the extracellular milieu. The matured protein without the signal peptide was predicted to be 23 kDa with a theoretical isoelectric point (pI) of 5.42. The PEBP domain was predicted to be from A^{50} to A^{196}.

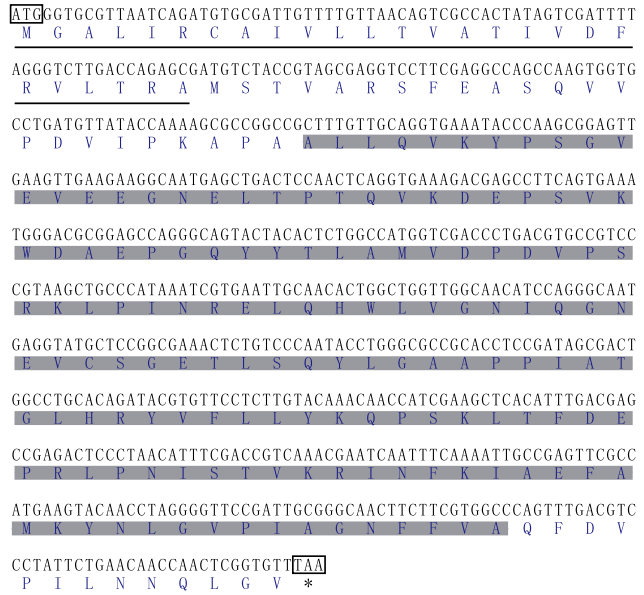

Fig. 1. Nucleotide sequence and deduced amino acid sequence of BmPEBP. The black border in the figure indicates the start codon (ATG) and stop codon (TAA). Numbers to the left of each row refer to the nucleotide or amino acid position. The putative signal peptide is underlined. The asterisk (*) indicates the stop codon. The PEBP domain predicted by the SMART program is shadowed.

Multiple-sequence alignment was performed to show evolutionarily or structurally related positions between BmPEBP and its homologs (Fig. 2). BmPEBP showed about 30–70% sequence identity with other proteins in the PEBP family (Supplementary File: Table S1). BmPEBP shared the greatest sequence identity (65%) with PxPEBP (GenBank ID: NP_001298632.1) from *Papilio polytes*. The D-P-D-X-P motif at position 95–110, the R-E-X-H-X-V motif at position 118–126, and the G-X-H-R motif at position 150–155 (numbering according to BmPEBP) are highly conserved for all the PEBPs. In particular, the conserved Pro^{106}, His^{121}, and His^{154} constitute the active binding site. Overall, PEBP proteins of all species are highly conserved in the “PEBP” domain region, particularly in the active binding site region. Insect PEBPs contain specific N-terminal sequences, which were predicted as signal peptides. However, PEBPs from mammals and plants lack signal peptides (Fig. 2). To further elucidate the phylogenetic relationship among PEBPs, 60 PEBP sequences (20 species each of insects, plants, and mammals) (Supplementary File: Table S2) were used to construct the phylogenetic tree. The PEBP phylogenetic tree was clearly clustered into three branches, separating insect PEBPs, plant PEBPs, and mammalian PEBPs (Fig. 3). By performing phylogenetic analysis on insect PEBPs, we can see that lepidoptera PEBPs were gathered well into one cluster (Supplementary File Fig. S4).

3.2. Protein expression and purification

To obtain the BmPEBP protein for biochemical analysis, soluble BmPEBP was expressed by using a prokaryotic expression system. We induced expression at 16 °C for 4 h, 12 h, 20 h, 28 h, and 36 h. As shown in Fig. 4A, a dominant protein band with a molecular mass of 27 kDa was detected in the BL21 cell supernatant at the 12 h, 20 h, 28 h, and 36 h (Fig. 4A). PEBP protein was purified effectively by Ni^{2+}-NTA affinity chromatography and gel filtration. SDS-PAGE indicated that purified BmPEBP was approximately 27 kDa (Fig. 4B), which is approximately consistent with its theoretical molecular weight of 23 kDa. The single eluted peak of the molecular sieve showed that BmPEBP was obtained with high purity (Fig. 4C).

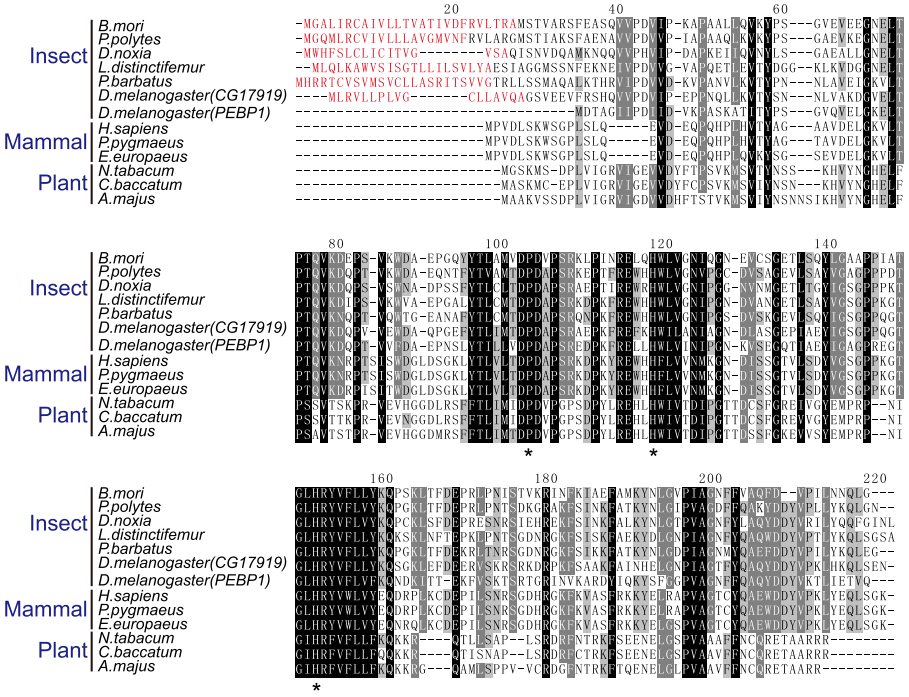

Fig. 2. Sequence analysis of PEBP homologs. Multiple sequence alignment with *Bombyx mori* BmPEBP (XP_004922749.1), PpPEBP from *Papilio polytes* (NP_001298632.1), DnPEBP from *Diuraphis noxia* (XP_015373613.1), LdPEBP from *Lethocerus distinctifemur* (ATU82444.1), PbPEBP from *Pogonomyrmex barbatus* (XP_011639892.1), DmPEBP2 (CG17919) from *Drosophila melanogaster* (CG17919), DmPEBP1 from *Drosophila melanogaster* (CG18594), HsPEBP from *Homo sapiens* (NP_002558.1), PpPEBP from *Pongo pygmaeus* (XP_004054017.1), EePEBP from *Erinaceus europaeus* (XP_007528723.1), NtPEBP from *Nicotiana tabacum* (XP_016494013.1), CbPEBP from *Capsicum baccatum* (PHT30106.1), and AmPEBP from *Antirrhinum majus* (Q41261.1). Alignments were performed with ClustalX. Red text indicates a signal peptide. Conserved, highly conserved, and identical amino acid residues are highlighted in light gray, gray, and black, respectively. "*" indicates an active binding site. (For interpretation of the references to color in this figure legend, the reader is referred to the Web version of this article.)

3.3. 3 secondary structure and physicochemical properties of BmPEBP

Far-UV CD spectroscopy revealed typical negative peak at 216 nm (Fig. 5A), indicating that BmPEBP had a well-defined β-sheet structure. The β-sheet content was calculated to be 41%, which was consistent with the secondary structure of BmPEBP predicted by Psipred (Supplementary Fig. S1).

To explore the effects of pH and temperature on the secondary structure of BmPEBP, buffers of various pH values and different temperatures were applied. The pH stability and thermal stability of BmPEBP were monitored by the θ_{216} shift in CD spectra. The results showed that BmPEBP was relatively stable in the pH range of 3–11 (Fig. 5B). When the pH was adjusted to near the isoelectric point of 5.42, expansion was rapidly induced in the β-sheet structure of BmPEBP. The structure of BmPEBP protein was stable in buffers with pH values far away from the isoelectric point (Fig. 5B). In terms of temperature, BmPEBP was relatively stable at 17.5–57.5 °C (Fig. 5C). When the temperature increased to 60 °C, the peak at 216 nm began to decay, suggesting that BmPEBP protein began to denature. At 72.5 °C, the peak almost disappeared, implying the nearly complete denaturation of the BmPEBP protein (Fig. 5C). The unfolding transition of BmPEBP induced by temperature was assumed to be a two-state model, with the midpoint of the unfolding curve representing the melting temperature (Tm) of BmPEBP. The thermal denaturation curve in Fig. 5D showed that the thermal unfolding of BmPEBP was a cooperative process. Tm, ΔH, and ΔS were calculated to be 62.27 °C ± 0.14 °C, 570.10 ± 0.17 kJ/mol, and 1.70 ± 0.03 KJ/(mol·K), respectively.

3.4. Three-dimensional structural characterization of BmPEBP

A structural model of BmPEBP was constructed based on the crystal structure of Tm16 from *Trichuris muris* (PDB: 5tvd) using SWISS-MODEL. The sequence identity between the template and BmPEBP was 54.14% (with 89% coverage), and the QMEAN Z-score was −1.64 for the model. The root-mean-square deviation between the model and 5tvd was 0.41 Å.

The overall structure of the homologous model showed that BmPEBP comprises eight β-sheets and three α-helices (Fig. 6A). The model shows that five β-sheets form a large central β-fold region, and the other three β-sheets form a small anti-parallel β-piece, which is assembled next to the central β-fold region. Among the three α-helices, one is located at the N-terminus, one is at the C-terminus, and the other one is assembled on one side of the central β-fold. The overall shape of BmPEBP is cylindrical, with a cross-shaped channel in the center (Fig. 6B), which is similar to previously reported mammalian PEBP structures. Multiple-sequence alignments and structural analyses showed that the active site of BmPEBP consists of conserved Pro^{106}, His^{121}, and His^{154} and is located at the bottom of the axial cross (Fig. 6C). The amine group of the basic residues faces the center of the tripod and produces a high positive charge in the active center to facilitate the binding of negatively charged group. We thus speculate that this region acts as an important ligand-binding region (Simister et al., 2002). It is interesting that bovine and human PEBPs can bind to many negatively charged ligands such as acetate, phosphate, and dimethyl arsenate, as well as the terminal group phosphoethanolamine of phosphatidylethanolamine (Banfield et al., 1998a; Simister et al., 2010).

3.5. Expression profiling of BmPEBP and upregulation of BmPEBP induced by microorganisms

The expression of *BmPEBP* in different tissues was analyzed by qPCR. Tissues were dissected out from larvae on day 3 of the fifth instar. Strong signals were detected in the silk glands, but very low expression was found in other tissues (Fig. 7A). These results showed that *BmPEBP* was highly and specifically expressed in the silk gland (Fig. 7A). qPCR was also employed to investigate the expression of *BmPEBP* in the larval fat body after infection with two kinds of fungi: *B. bassiana* and *C. albicans*. The *BmPEBP* gene was found to be significantly upregulated at 6 h after infection with *B. bassiana* compared to the PBS control, and significantly upregulated at 6 and 24 h after infection with *C. albicans* compared to the PBS control (Fig. 7C). Meanwhile, two kinds of bacteria, *E. coli* and *S. aureus*, were also used to infect silkworm larvae by injection. The qPCR results showed that *BmPEBP* had no obvious upregulation in the fat body after *E. coli* infection (Fig. S2A), while *BmPEBP* was significantly upregulated 12 and 18 h after *S. aureus*

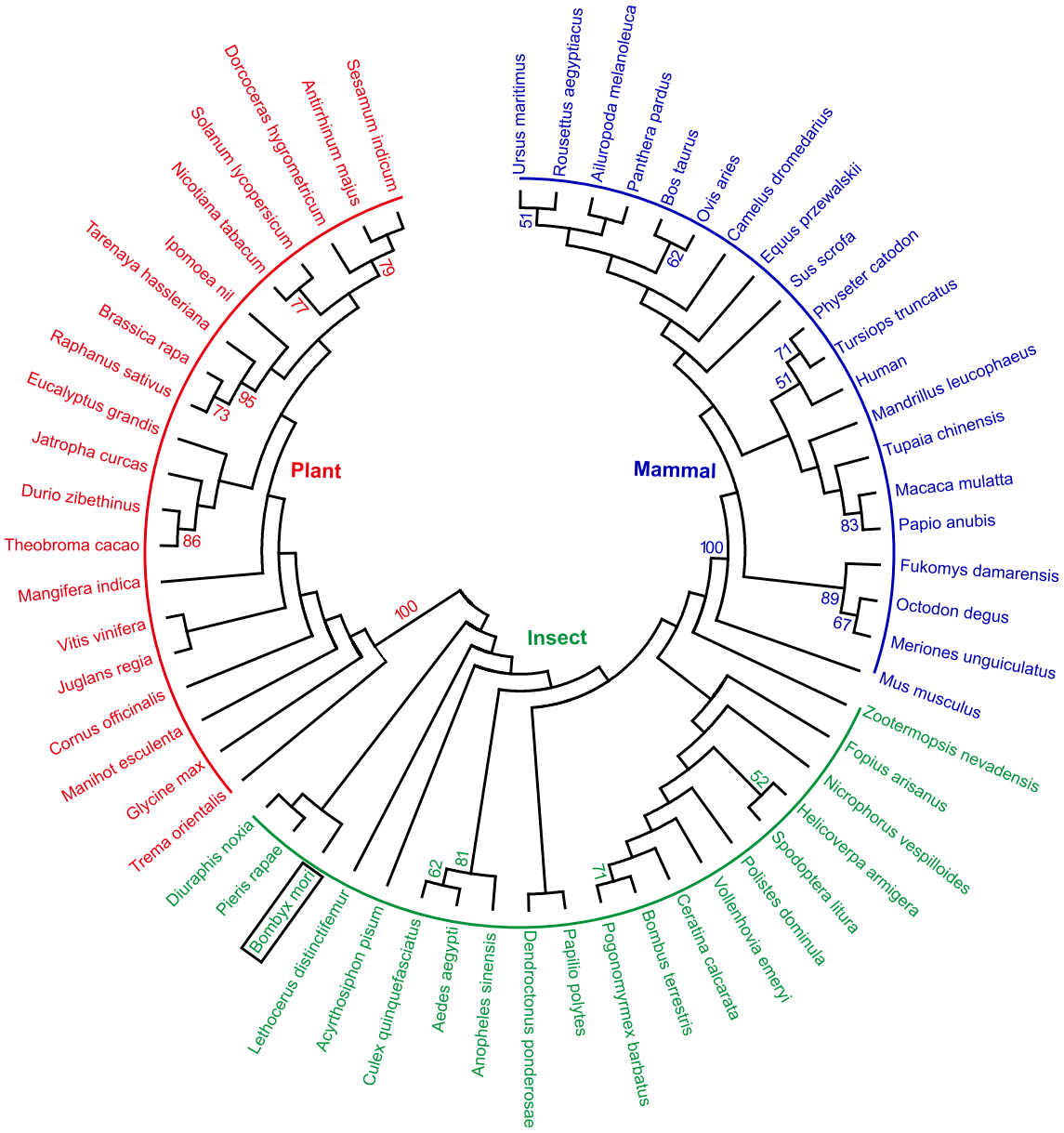

Fig. 3. Phylogenetic tree of PEBPs from insect species, plant species, and mammal species. BmPEBP is highlighted with a black box.

infection (Fig. S2B).

3.6. Inhibitory activity of recombinant BmPEBP

To investigate the type of proteases that could be suppressed by recombinant BmPEBP, various proteases were used in *vitro* tests (Fig. S3). BmPEBP barely suppressed microbial proteases, such as subtilisin A from *Bacillus licheniformis* and protease K from *Tritirachium album*, and it could not inhibit bovine pancreatic trypsin or bovine pancreatic chymotrypsin.

3.7. In vitro antimicrobial activity of BmPEBP

To evaluate the inhibitory activity of BmPEBP against fungi, the spores of *S. cerevisiae*, *C. albicans*, *B. bassiana*, and *A. fumigatus* were incubated with 0.1 mg/mL of recombinant BmPEBP. The growth curve of fungal spores was monitored by UV spectrophotometry. As shown in Fig. 8A–D, BmPEBP showed significant growth inhibitory activity against the fungal spores of *A. fumigatus*, *B. bassiana*, *S. cerevisiae*, and *C. albicans*. The inhibitory activity of BmPEBP against *A. fumigatus* and *B. bassiana* was higher than that against *S. cerevisiae* and *C. albicans* (Fig. 8E–H). We also incubated *E. coli* and *S. aureus* with 0.1 mg/mL of recombinant BmPEBP. The growth curve of the bacteria monitored by UV spectrophotometry showed that BmPEBP did not inhibit the growth of either bacterial species (Figure S2 C–D).

4. Discussion

Studies on PEBP1 in *D. melanogaster* have established that PEBP1 helps hosts resist exogenous microbes (Reumer et al., 2009). Amino acid sequence analysis of BmPEBP indicated that BmPEBP has a “PEBP” domain, similar to the PEBP1 of *D. melanogaster* (Reumer et al., 2009). Recent research has also identified PEBPs in the silk glands and silk fibers from two lepidopteran insects, *S. derogata* and *B. mori* (Dong et al., 2013; Su et al., 2015). Therefore, in this study, we systematically analyzed the sequence evolution, structural characterization, expression pattern, and antifungal activity of BmPEBP.

Multiple-sequence alignment was performed to identify structurally

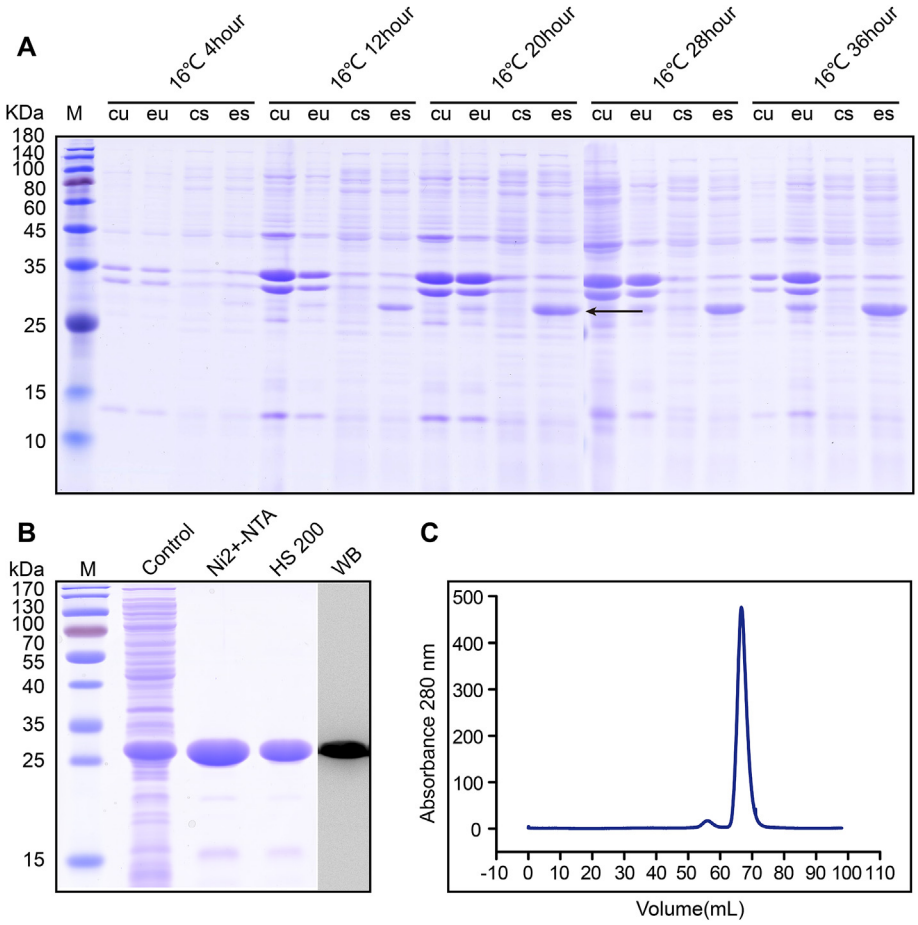

Fig. 4. Prokaryotic expression and purification of PEBP. (A) Reduced SDS-PAGE analyses of target protein expression in different conditions. "M" indicates the molecular weight standards. "cu" and "eu" represent the control unsolubilized component and experimental unsolubilized component, respectively; "cs" and "es" represent the control supernatant and experiment supernatant, respectively. Uninduced *E. coli* BL21 (DE3) was used as the control. *E. coli* BL21 (DE3) was induced with 0.1 mM IPTG at 16 °C for 20 h or at 37 °C for 4 h. The arrow shows the recombinant PEBP. (B) SDS-PAGE analysis of the purified BmPEBP protein. M: marker, Control: stock solution after ultrasonication, Ni^{2+}-NTA: nickel affinity chromatography column, HS-200, molecular sieve for purification, and WB: western blot. (C) Purification of the recombinant BmPEBP by gel filtration.

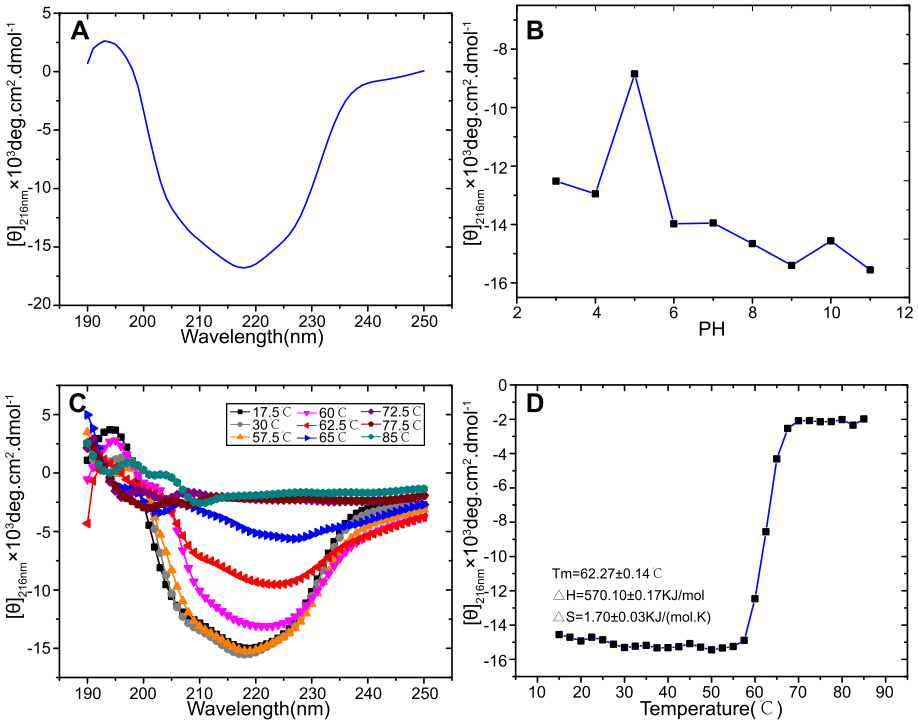

Fig. 5. The secondary structure and stability study of BmPEBP. (A) Circular dichroism spectrum of BmPEBP. (B) Conformational changes of BmPEBP in pH 3–11 buffers. (C) The secondary conformational profiles of BmPEBP in the range of 15–82.5 °C. (D) Conformational changes in BmPEBP induced by temperature. Mean residue ellipticities at 216 nm were used to monitor the conformational changes of BmPEBP induced by pH and temperature.

conserved residues in the BmPEBP and among the homologs, which showed the conserved region was from the 70th amino acid residues to the 200th residues. Three predicted active sites of PEBPs are highly conserved and located in this region (Banfield and Brady, 2000b). Moreover, phylogenetic analysis indicated that the PEBP family of proteins appears to be very conservative in evolution. Insect PEBP

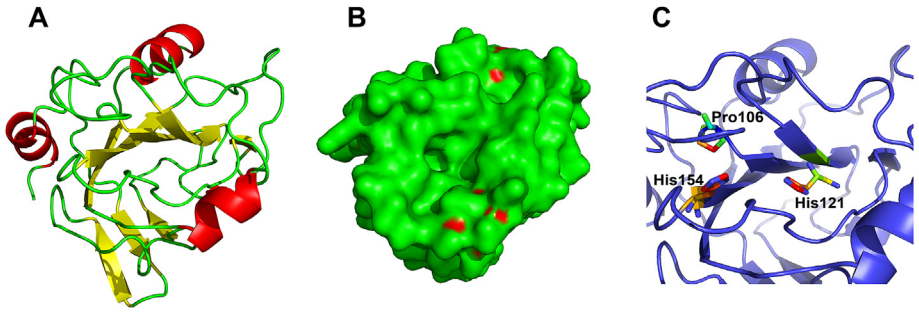

Fig. 6. The overall structure of BmPEBP. (A) Cartoon representation of the fold in BmPEBP. Red, α-helical structure; yellow, β-folded structure; green, random coil structure. (B) Surface electric potential of BmPEBP, showing a substrate-binding pocket in the β-sheet domain. (C) The active binding site at the bottom of the substrate-binding pocket. Residues are shown in colorful stick format. (For interpretation of the references to color in this figure legend, the reader is referred to the Web version of this article.)

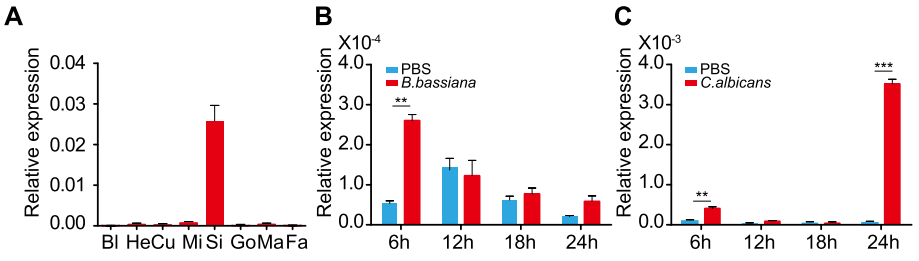

Fig. 7. The mRNA expression levels of *BmPEBP*. (A) The mRNA expression level of *BmPEBP* in different tissues from day 3 of the fifth instar. The relative mRNA expression levels of *BmPEBP* in the fat bodies of *B. bassiana*-infected (B) and *C. albicans*-infected (C) larvae at different time points. The y-axis indicates the relative expression level of *BmPEBP* mRNA transcripts. Student's *t*-test was used to evaluate statistical significance. Vertical bars represent the mean ± SE (n = 3). **p < 0.001 and *p < 0.01 versus control. Error bars indicate the standard error of the mean (n = 3).

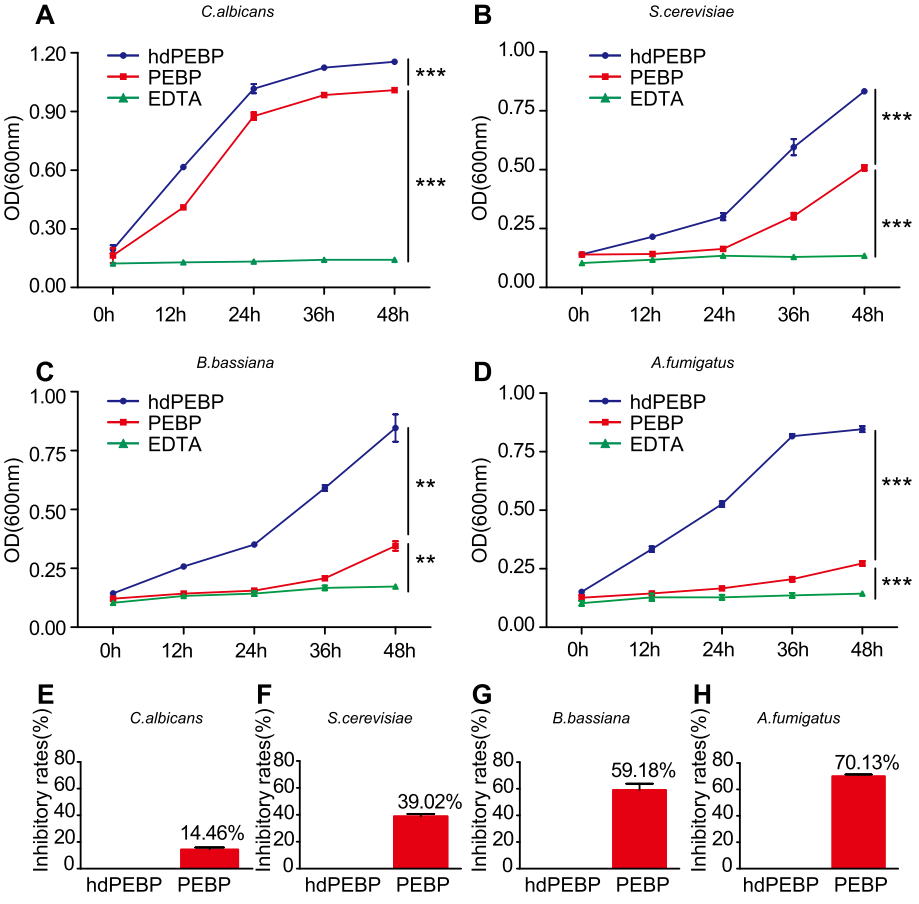

Fig. 8. Antifungal activity of BmPEBP. (A) Inhibitory effect of BmPEBP on the growth of *C. albicans*. (B) Inhibitory effect of BmPEBP on the growth of *S. cerevisiae*. (C) Inhibitory effect of BmPEBP on the growth of *B. bassiana*. (D) Inhibitory effect of BmPEBP on the growth of *A. fumigatus*. (E) Inhibitory effect of BmPEBP on *C. albicans* growth at 48 h. (F) Inhibitory effect of BmPEBP on *S. cerevisiae* growth at 48 h. (G) Inhibitory effect of BmPEBP on *B. bassiana* growth at 48 h. (H) Inhibitory effect of BmPEBP on *A. fumigatus* growth at 48 h. Student's *t*-test was used to evaluate statistical significance. Vertical bars represent the mean ± SE (n = 3). **p < 0.001 and *p < 0.01 versus control. Error bars indicate the standard error of the mean (n = 3).

sequences and mammalian PEBP sequences are more similar to each other than to plant PEBP sequences.

Secondary structure analysis revealed that BmPEBP was mainly composed of β-sheets and random coils, as well as a small amount of α-helices. These characteristics are particularly similar to the structural features known for human, bovine, and plant PEBPs (Vallée et al., 2010). It is noteworthy that the C-terminal of bovine PEBP corresponds to the helical region of the C-terminal peptide, which is close to the presumed ligand-binding site in the whole PEBP (Banfield et al., 1998a; Bernier et al., 1986). Our study also found that the C-terminal structure of BmPEBP is very similar to that of PEBP in cattle and other mammals. Structural analyses showed that the conserved active site, consisting of conserved Pro[96], His[111], and His[143], is located at the bottom of the axial tripod. We thus speculate that the roles of BmPEBP in immunity might

be related with its binding abilities with small lipid molecules such as phospholipids.

It has been reported from previous studies that there are two types of PEBPs in insects, one is intracelular PEBP without signal peptide and the other is secretory PEBP with signal peptide (Reumer et al., 2009). Studies in *D. melanogaster* showed that PEBP without a signal peptide has similar function with mammalian PEBPs, which were involved in activation of the immune response pathway (Anette W. Bruun et al., 1998; Vierstraete et al., 2004). In mammals, intracellular PEBPs bind to Raf-1 to interfere with the pathways downstream of the MAPK pathway (Schubbert et al., 2007; Yeung et al., 2000). In addition, it is involved in the regulation of the NF-κB signaling pathway (Li et al., 2007; Yeung et al., 2001). PEBP also inhibits GRK-2 activity to enhance G-protein-coupled receptor signaling (Lorenz et al., 2003). *D. melanogaster* PEBP proteins were detected in hemolymph and fat body (Reumer et al., 2009; Vierstraete et al., 2004). Due to that many evidence showed that PEBPs might be related to the innate immune defense in insects (Guedes et al., 2003; Karlsson et al., 2004; Vierstraete et al., 2004). Thus, we focus on the immune role of silkworm PEBP. PEBP1 in *D. melanogaster* is involved in mediating the innate immune response, and PEBP1 over-expression can help *D. melanogaster* larvae resist bacterial infection and improve the larval survival rate (Levy et al., 2004; Reumer et al., 2009; Vierstraete et al., 2004). However, no evidence showed that *D. melanogaster* PEBP1 can directly inhibit bacterial growth. *D. melanogaster* PEBP1 may exert function by activating immune pathways (Agaisse and Perrimon, 2010; Arbouzova and Zeidler, 2006; Dostert et al., 2005). The BmPEBP identified in the silkworm has predicted signal peptide, indicated it is a secretory protein, which is synthesized in the silk gland and secreted into cocoon silk. Previous studies also identified BmPEBP protein in the silk by the proteomics approach (Dong et al., 2013). PEBP has been also found to be expressed in the silk gland of *S. derogata* (Lepidoptera: *Pyralidae*) (Su et al., 2015). This study suggested that BmPEBP act an antimicrobial protein in the silk. In fact, silkworm cocoon silk are key fortifications for silkworm pupae, which not only protect against external physical damage but also resist microbial invasion. Studies have revealed the presence of many antimicrobial proteins in the cocoon silk. These antimicrobial mechanisms have been studied in detail, including SPI38, SPI39, BmGlv2, Seroin1, and Seroin2 (Li et al., 2012, 2015b; Singh et al., 2014; Wang et al., 2018; Zurovec et al., 1998). The antifugal activity of BmPEBP was reported for the first time in this study. The inhibitory mechanism of BmPEBP against fungi still needed to be further studied.

Acknowledgments

This work was supported by the National Natural Science Foundation of China (No. 31530071, 31702184 and 31772532), the Fundamental Research Funds for the Central Universities of China (No. XDJK2018C011), the PhD Start-up Foundation of Southwest University (No. swu115049 and swu116076), and the 2017 Special Grants Program for National Cocoon Silk Development (No. GJ2017JSB001).

Appendix A. Supplementary data

Supplementary data to this article can be found online at https://doi.org/10.1016/j.ibmb.2019.03.011.

References

Agaisse, H., Perrimon, N., 2010. The roles of JAK/STAT signaling in Drosophila immune responses. Immunol. Rev. 198, 72–82.
Arbouzova, N.I., Zeidler, M.P., 2006. JAK/STAT signaling in Drosophila: insights into conserved regulatory and cellular functions. Development 133, 2605–2616.
Banfield, M., Brady, R., 2000a. The structure of Antirrhinum centroradialis protein (CEN) suggests a role as a kinase regulator. J. Mol. Biol. 297, 1159–1170.
Banfield, M.J., Brady, R.L., 2000b. The structure of Antirrhinum centroradialis protein (CEN) suggests a role as a kinase regulator. J. Mol. Biol. 297, 1159–1170.
Banfield, M.J., Barker, J.J., Perry, A.C., Brady, R.L., 1998a. Function from structure? The crystal structure of human phosphatidylethanolamine-binding protein suggests a role in membrane signal transduction. Structure 6, 1245.
Banfield, M.J., Barker, J.J., Perry, A.C., Brady, R.L., 1998b. Function from structure? The crystal structure of human phosphatidylethanolamine-binding protein suggests a role in membrane signal transduction. Structure 6, 1245–1254.
Bernier, I., Jollès, P., 1984. Purification and characterization of a basic 23 kDa cytosolic protein from bovine brain. Biochim. Biophys. Acta Protein Struct. Mol. Enzymol. 790, 174–181.
Bernier, I., Tresca, J.P., Jollès, P., 1986. Ligand-binding studies with a 23 kDa protein purified from bovine brain cytosol. Biochim. Biophys. Acta 871, 19–23.
Bradley, D., Ratcliffe, O., Vincent, C., Carpenter, R., Coen, E., 1997. Inflorescence commitment and architecture in arabidopsis. Science 275, 80–83.
Bruun, Anette W., Svendsen, Ib, Susanne, O., Sørensen, Winther, Jakob R., 1998. A high-affinity inhibitor of yeast carboxypeptidase Y is encoded by TFS1 and shows homology to a family of lipid binding proteins. Biochemistry 37, 3351–3357.
Dong, Z., Zhao, P., Wang, C., Zhang, Y., Chen, J., Wang, X., Lin, Y., Xia, Q., 2013. Comparative proteomics reveal diverse functions and dynamic changes of Bombyx mori silk proteins spun from different development stages. J. Proteome Res. 12, 5213–5222.
Dostert, C., Jouanguy, E., Irving, P., Troxler, L., Galianaarnoux, D., Hetru, C., Hoffmann, J.A., Imler, J.L., 2005. The Jak-STAT signaling pathway is required but not sufficient for the antiviral response of drosophila. Nat. Immunol. 6, 946.
Gems, D., Ferguson, C.J., Robertson, B.D., Nieves, R., Page, A.P., Blaxter, M.L., Maizels, R.M., 1995. An abundant, trans-spliced mRNA from Toxocara canis infective larvae encodes a 26-kDa protein with homology to phosphatidylethanolamine-binding proteins. J. Biol. Chem. 270, 18517–18522.
Gibbons, R., Adeoya-Osiguwa, S.A., Fraser, L.R., 2005. A mouse sperm decapacitation factor receptor is phosphatidylethanolamine-binding protein 1. Reproduction 130, 497–508.
Guedes, S.D.M., Rui, V., Tomer, K., Domingues, M.R.M., Correia, A.J.F., Amado, F., Domingues, P., 2003. Drosophila melanogaster larval hemolymph protein mapping. Biochem. Biophys. Res. Commun. 312, 545–554.
Guo, X., Dong, Z., Zhang, Y., Li, Y., Liu, H., Xia, Q., Zhao, P., 2016. Proteins in the cocoon of silkworm inhibit the growth of Beauveria bassiana. PLoS One 11, e0151764.
Hengst, U., Albrecht, H., Hess, D., Monard, D., 2001. The phosphatidylethanolamine-binding protein is the prototype of a novel family of serine protease inhibitors. J. Biol. Chem. 276, 535–540.
Karlsson, C., Korayem, A.M., Scherfer, C., Loseva, O., Dushay, M.S., Theopold, U., 2004. Proteomic analysis of the Drosophila larval hemolymph clot. J. Biol. Chem. 279, 52033–52041.
Keller, E.T., Fu, Z., Brennan, M., 2004. The role of Raf kinase inhibitor protein (RKIP) in health and disease. Biochem. Pharmacol. 68, 1049–1053.
Levy, F., Bulet, P., Ehret-Sabatier, L., 2004. Proteomic analysis of the systemic immune response of drosophila. Biochimie 86, 607–616.
Li, H., Wang, X., Li, N., Qiu, J., Zhang, Y., Cao, X., 2007. hPEBP4 resists TRAIL-induced apoptosis of human prostate cancer cells by activating Akt and deactivating ERK1/2 pathways. J. Biol. Chem. 282, 4943.
Li, Y., Zhao, P., Liu, S., Dong, Z., Chen, J., Xiang, Z., Xia, Q., 2012. A novel protease inhibitor in Bombyx mori is involved in defense against Beauveria bassiana. Insect Biochem. Mol. Biol. 42, 766–775.
Li, Y., Zhao, P., Liu, H., Guo, X., He, H., Zhu, R., Xiang, Z., Xia, Q., 2015a. TIL-type protease inhibitors may be used as targeted resistance factors to enhance silkworm defenses against invasive fungi. Insect Biochem. Mol. Biol. 57, 11–19.
Li, Y.S., Liu, H., Zhu, R., Xia, Q.Y., Zhao, P., 2015b. Protease inhibitors in Bombyx mori silk might participate in protecting the pupating larva from microbial infection. Insect Sci. 23, 835–842.
Lorenz, K., Lohse, M.J., Quitterer, U., 2003. Protein kinase C switches the Raf kinase inhibitor from Raf-1 to GRK-2. Nature 426, 574.
Mima, J., Hayashida, M., Fujii, T., Narita, Y., Hayashi, R., Ueda, M., Hata, Y., 2005. Structure of the carboxypeptidase Y inhibitor IC in complex with the cognate proteinase reveals a novel mode of the proteinase-protein inhibitor interaction. J. Mol. Biol. 346, 1323–1334.
Ojika, K., 2000. [Hippocampal cholinergic neurostimulating peptide]. Prog. Neurobiol. 60, 37–83.
Pikielny, C.W., Hasan, G., Rouyer, F., Rosbash, M., 1994. Members of a family of Drosophila putative odorant-binding proteins are expressed in different subsets of olfactory hairs. Neuron 12, 35–49.
Reumer, A., Bogaerts, A., Van, L.T., Husson, S.J., Temmerman, L., Choi, C., Clynen, E., Hassan, B., Schoofs, L., 2009. Unraveling the protective effect of a Drosophila phosphatidylethanolamine-binding protein upon bacterial infection by means of proteomics. Dev. Comp. Immunol. 33, 1186–1195.
Schubbert, S., Shannon, K., Bollag, G., 2007. Hyperactive Ras in developmental disorders and cancer. Nat. Rev. Canc. 7, 295–308.
Simister, P.C., Banfield, M.J., Brady, R.L., 2002. The crystal structure of PEBP-2, a homologue of the PEBP/RKIP family. Acta Crystallogr. 58, 1077–1080.
Simister, P.C., Banfield, M.J., Brady, R.L., 2010. The crystal structure of PEBP-2, a homologue of the PEBP/RKIP family. Acta Crystallogr. 58, 1077–1080.
Singh, C.P., Vaishna, R.L., Kakkar, A., Arunkumar, K.P., Nagaraju, J., 2014. Characterization of antiviral and antibacterial activity of Bombyx mori seroin proteins. Cell Microbiol. 16, 1354–1365.
Su, H., Cheng, Y., Wang, Z., Li, Z., Stanley, D., Yang, Y., 2015. Silk gland gene expression during larval-pupal transition in the cotton leaf roller Sylepta derogata (Lepidoptera: Pyralidae). PLoS One 10, e0136868.
Tohdoh, N., Tojo, S., Agui, H., Ojika, K., 1995. Sequence homology of rat and human HCNP precursor proteins, bovine phosphatidylethanolamine-binding protein and rat

23-kDa protein associated with the opioid-binding protein. Mol. Brain Res. 30, 381–384.
Trottein, F., Cowman, A.F., 1995. The primary structure of a putative phosphatidylethanolamine-binding protein from Plasmodium falciparum ☆. Mol. Biochem. Parasitol. 70, 235–239.
Vallée, B., Teyssier, C., Maget-Dana, R., Ramstein, J., Bureaud, N., Schoentgen, F., 2010. Stability and physicochemical properties of the bovine brain phosphatidylethanolamine-binding protein. FEBS J. 266, 40–52.
Vierstraete, E., Verleyen, P., Baggerman, G., D'Hertog, W., Van, d.B.G., Arckens, L., De, L.A., Schoofs, L., 2004. A proteomic approach for the analysis of instantly released wound and immune proteins in Drosophila melanogaster hemolymph. In: Proceedings of the National Academy of Sciences of the United States of America, vol 101. pp. 470–475.
Wang, Q., Guo, P., Wang, Z., Liu, H., Zhang, Y., Jiang, S., Han, W., Xia, Q., Zhao, P., 2018. Antibacterial mechanism of Gloverin2 from silkworm. Int. J. Mol. Sci. 19.
Yeung, K., Janosch, P., Mcferran, B., Rose, D.W., Mischak, H., Sedivy, J.M., Kolch, W., 2000. Mechanism of suppression of the Raf/MEK/extracellular signal-regulated kinase pathway by the raf kinase inhibitor protein. Mol. Cell Biol. 20, 3079–3085.
Yeung, K.C., Rose, D.W., Dhillon, A.S., Yaros, D., Gustafsson, M., Chatterjee, D., Mcferran, B., Wyche, J., Kolch, W., Sedivy, J.M., 2001. Raf kinase inhibitor protein interacts with NF-κB-Inducing kinase and TAK1 and inhibits NF-κB activation. Mol. Cell Biol. 21, 7207–7217.
Zhang, Y., Zhao, P., Dong, Z., Wang, D., Guo, P., Guo, X., Song, Q., Zhang, W., Xia, Q., 2015. Comparative proteome analysis of multi-layer cocoon of the silkworm, Bombyx mori. PLoS One 10, e0123403.
Zurovec, M., Yang, C., Kodrík, D., Sehnal, F., 1998. Identification of a novel type of silk protein and regulation of its expression. J. Biol. Chem. 273, 15423–15428.